Research article

Analysis of composite concrete steel column using "X" shape steel section

Ahmad Zeyad Abu Sharea [*], Shideh Shadravan

The University of Oklahoma, Norman, OK, USA

ARTICLE INFO

ABSTRACT

In this paper, a new structural steel shape is proposed to be used in composite columns. The model is made of a concrete column with the proposed steel section embedded in concrete with four angles "L shape", welded together to form the shape "X". The equivalent compressive strength capacity of this "X" shape was compared to the conventional steel "W shape" section. The main goal of the research is the strength enlargement of composite columns.

Three 6 ft long columns were analyzed: one conventional "W" section (W100 × 330), one with two angles (2 L 89 × 76.5 × 8), and one with four angles (4 L 50 × 50 × 6.5). Finite element analysis was completed using ABAQUS software and theoretical analysis was performed using AISC and Eurocode4. The deflection control analysis using ABAQUS was validated first on samples from a previously published experimental study conducted in the laboratory, and results from ABAQUS were aligned with the experimental study outcomes.

This study found that the proposed "X" shape steel section has comparable compressive strength values to the conventional "W" section.

1. Introduction

The demand for cost-effective construction materials has increased in recent years, due to the development of quick and intelligent construction processes. Composite concrete elements are now frequently used, especially in high-rise buildings [1]. To meet high-strength column capacity requirements, a column with large concrete section is necessary, which reduces the available living space in the floor. Larger sections are more expensive, and less spacious floor areas are undesirable. By using composite concrete elements, the regular reinforced concrete column is replaced, and the cross-sectional area is reduced, sustaining acceptable floor areas, a smaller cross-sectional area, and higher strength capacity [2,3].

Generally, a steel-concrete composite column refers to a concrete-encased hot-rolled steel section ("I" or "W" sections), or a concrete-filled tubular section of hot-rolled steel. The most common section is the "W" section, which has been described as the "undisputed star of the steelwork" [4].

Several researchers have studied the steel sections in AISC manual [5] with various concrete strengths and cross-sections, focusing on compressive and flexural strength along with shear resistance [6–9], and [10]. In the aforementioned studies, stress-strain and force-moment diagrams were drawn to compare theoretical and experimental results to find similarities and consistency. Furthermore, theoretical analyses for steel sections were conducted based on two main codes: Eurocode 4 and AISC [5,11].

Eurocode 4 [11] provides more accurate experimental results than conservative AISC results (Ellobody & Young [12], and Ellobody et al. [13]). Finite elements analysis was strongly used in many studies to simulate the behavior of structural elements and compare it with theoretical or experimental data [2,14].

This paper investigates an increase in strength capacity using a newly proposed "X" shape steel section, with four angles representing the shape "X" since the "X" shape was never proposed or created before. The idea of the shape "X" as a steel section came from its geometry. According to AISC [5] conventions, compressive strength calculations in columns should be considered on a major (strong) x-axis and a minor (weak) y-axis to prevent a potential failure due to weak axis geometric properties. The "X" shape has symmetrical dimensions, which helps in column strength and eliminating having two axes: strong and weak axes (X, Y). This paper aims to compare the symmetrical "X shape" with the asymmetrical conventional "W shape" steel section by running a theoretical analysis using AISC and Eurocode 4 and software simulation using ABAQUS to verify if the proposed section can be presented as an alternative section to the conventional "W" steel sections.

2. Material and methods

Four methods were applied in this paper, three main analysis methods were used to study the proposed steel "X" section and compare it to conventional steel sections as following: two theoretical analysis using methods of calculating the axial compressive force in AISC manual [5] and Eurocode [11], and software analysis using finite element method by ABAQUS [15]. Fourth method is validating previous published results where ABAQUS and field testing were done [16] on similar sections as described in the following section 2.1.

2.1. Validation of pervious published results [16]

The numerical simulation to be used in ABAQUS for the proposed steel section "X" is validated using an experimental specimen from a previous study conducted by Rahman, Begum and Ahsan Rahman, Begum and Ahsan [16]. Three fully encased composite columns were tested, and nonlinear large-displacement 3D finite element models of these columns are separately developed in ABAQUS software [15] to investigate their behavior and strength.

In the study by Rahman, Begum and Ahsan paper [16], Three different shapes of the structural steel section are used in the specimens i.e., H, cross and I shaped sections, as illustrated in Fig. 1 below, where Fig. 1 (a) is showing a fully encased column FEC with "H" section, Fig. 1 (b) is showing an FEC with two "I" sections, and Fig. 1 (c) is showing am FEC with one "I" section. All specimens have a square cross-section of 280 × 280 mm and a constant length of 1200 mm. All specimens' properties are described in Figs. 2–4.

Figs. 5–7 below depicts the elements of columns SCR1, SCR4 and SCR7 in ABAQUS and a comparison result obtained from the numerical simulation and the result from experimental test [16]. Fig. 8 demonstrates the experimental curve in blue dotted line, and the numerical curve in black continuous line for column SCR1.

As shown in Fig. 8 above, there is a good agreement between the experimental and numerical results in the pre and post peak in load for column SCR1.

Columns SCR4 and SCR7 comparison results were made by numbers as shown in Tables 1 and 2 below, the peak load and the axial deformation at the peak load are evaluated from both numerical simulation and experimental test under the applied axial load. The results of the comparison show a good agreement between the experimental and numerical results.

3. Theory and calculation

This paper studied three columns, each with a concrete cross-section of 200 mm by 200 mm and a length of 1830 mm. All specimens had four axial rebars of #10 mm, and all steel sections in each column were positioned in the center. The column section dimensions were chosen to have a failure load of less than 1333 KN, which is the maximum load that can be applied at the University of Oklahoma Fears laboratory in case of conducting future experimental. Table 3 and Fig. 9 below, show the section cross-section of each specimen, where Fig. 9 (a) shows the first specimen of a conventional composite concrete steel column CCSC with a "W" steel column embedded, Fig. 9 (b) shows an identical concrete column dimensions of a CCSC with two steel angles "L" embedded, and Fig. 9 (c) shows another
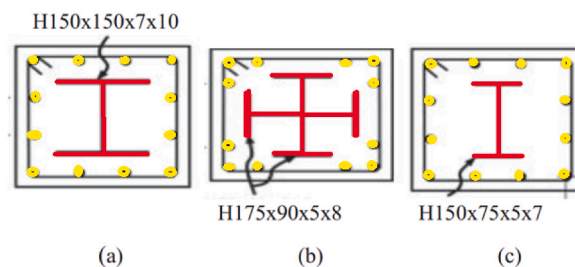

Fig. 1. Cross sections of FEC "fully encased column" with (a) H section of 150 × 150 × 7x10 mm, (b) two I sections of 175 × 90 × 5x8 mm and (c) one I section of 150 × 75 × 5 × 7. (1 mm = 0.04in).

| Specimen Designation | Size | | Length of Column | Structural Steel | | Tie Spacing (mm) |
	B (mm)	D (mm)	(mm)	Shape	Size (b_f x d x t_w) (mm)	
SRC1	280	280	1200	H	H150x150x7x10	φ-8mm @140
SRC2	280	280	1200	H	H150x150x7x10	φ-8mm @ 75
SRC3	280	280	1200	H	H150x150x7x10	φ-8mm @ 35
SRC4	280	280	1200	Cross	Two H175X90X5X8	φ-8mm @140
SRC5	280	280	1200	Cross	Two H175X90X5X8	φ-8mm @ 75
SRC6	280	280	1200	Cross	Two H175X90X5X8	φ-8mm @ 35
SRC7	280	280	1200	I	H150x75x5x7	φ-8mm @140
SRC8	280	280	1200	I	H150x75x5x7	φ-8mm @ 75
SRC9	280	280	1200	I	H150x75x5x7	φ-8mm @ 140
SRC10	280	280	1200	I	H150x75x5x7	φ-8mm @ 75

Fig. 2. Geometric properties of reference specimens [16]. (1 mm = 0.04in).

| Specimen Designation | Properties of concrete | | | | Properties of Steel Plate | | | | | |
	f_{cu} MPa	E_c MPa	ε_{cu} με	γ	F_y (MPa)	F_{sh} (MPa)	F_u (MPa)	ε_y (%)	ε_{sh} (%)	ε_u (%)
SRC 1	29.5	24932	1896	0.18	296	296	373	0.17	1.67	14
SRC 2	28.1	24499	1868	0.18	296	296	373	0.17	1.67	14
SRC 3	29.8	25023	1902	0.18	296	296	373	0.17	1.67	14
SRC 4	29.8	25023	1902	0.18	345	345	431	0.18	1.87	15
SRC 5	29.8	25023	1902	0.18	345	345	431	0.18	1.87	15
SRC 6	29.5	24932	1896	0.18	345	345	431	0.18	1.87	15
SRC 7	28.1	24499	1868	0.18	303	303	379	0.19	1.95	17
SRC 8	26.4	24997	1834	0.18	303	303	379	0.19	1.95	17
SRC 9	28.1	24449	1868	0.18	303	303	379	0.19	1.95	17
SRC 10	29.8	25023	1902	0.18	303	303	379	0.19	1.95	17

Fig. 3. Properties of concrete and steel sections [16]. (1 MPa = 0.145 Ksi).

CCSC with 4 steel angles "L" embedded.

3.1. Theoretical analysis method (AISC)

AISC 360 (chapter I, section 12) [5], equations "1" and "2" are used to calculate the design compressive strength ØcPn, and allowable compressive strength Pn/Ωc for axially loaded encased composite members for the three specimens.

Øc = 0.75 (LRFD), Ωc = 2.00 (ASD).

When Pno/Pe ≤ 2.25

$$Pn = Pno * \left(0.658^{(Pno/Pe)}\right)$$ Eq. (1)

When Pno/Pe > 2.25

$$Pn = 0.877 * Pe$$ Eq. (2)

Where:

| Specimen Designation	Properties of concrete				Properties of Rebar's				
	f_{cu}	E_c	ε_{cu}	F_y	F_{sh}	F_u	ε_y	ε_{sh}	ε_u
	MPa	MPa	με	(MPa)	(MPa)	(MPa)	(%)	(%)	(%)
SRC 1	29.5	24932	1896	350	350	438	0.24	1.95	15
SRC 2	28.1	24499	1868	350	350	438	0.24	1.95	15
SRC 3	29.8	25023	1902	350	350	438	0.24	1.95	15
SRC 4	29.8	25023	1902	350	350	438	0.25	2.21	14
SRC 5	29.8	25023	1902	350	350	438	0.25	2.21	14
SRC 6	29.5	24932	1896	350	350	438	0.25	2.21	14
SRC 7	28.1	24499	1868	350	350	438	0.26	2.24	16
SRC 8	26.4	24997	1834	350	350	438	0.26	2.24	16
SRC 9	28.1	24449	1868	350	350	438	0.26	2.24	16
SRC 10	29.8	25023	1902	350	350	438	0.26	2.24	16

Fig. 4. Properties of concrete and steel rebar's [16].
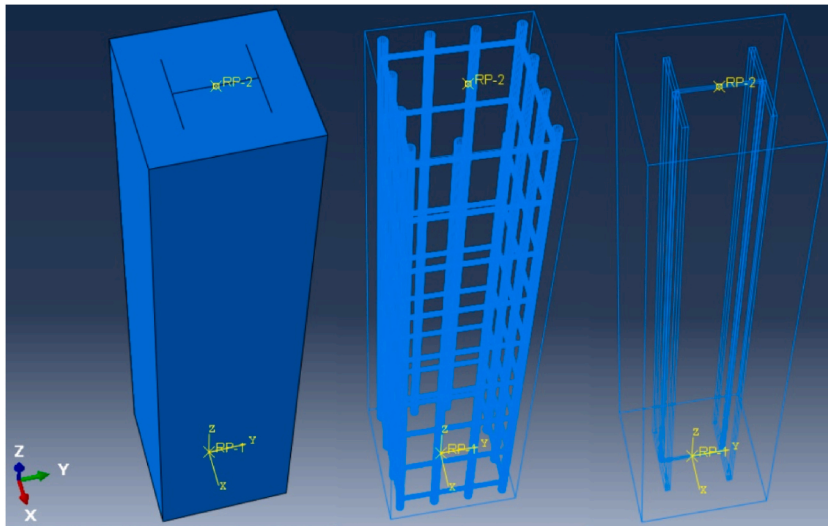
Fig. 5. View of the numerical model of SCR1.

$$Pno = Fy * As + Fysr * Asr + 0.85 * fc^{'} * Ac$$

AISC equations are explained more in Appendix A.

3.2. Theoretical analysis method (Eurocode4)

Eurocode4 section 6.7, equation "3" is used to calculate the plastic resistance to compression for encased concrete-encased composite members Npl, Rd.

$$Npl, Rd = Aa * fyd + 0.85 * Ac * fcd + As * fsd \qquad \text{Eq. (3)}$$

3.3. Software analysis (finite element ABAQUS)

Finite element analysis was performed using ABAQUS software to apply an axial concentric load on the three specimens and draw force-deflection graph, following the same methodology described in section 2.1. All angles of "L" section were assumed to form an "X" shape, with the dimensions of the angles equivalent to those used in the theoretical analysis. The force-deflection graphs were
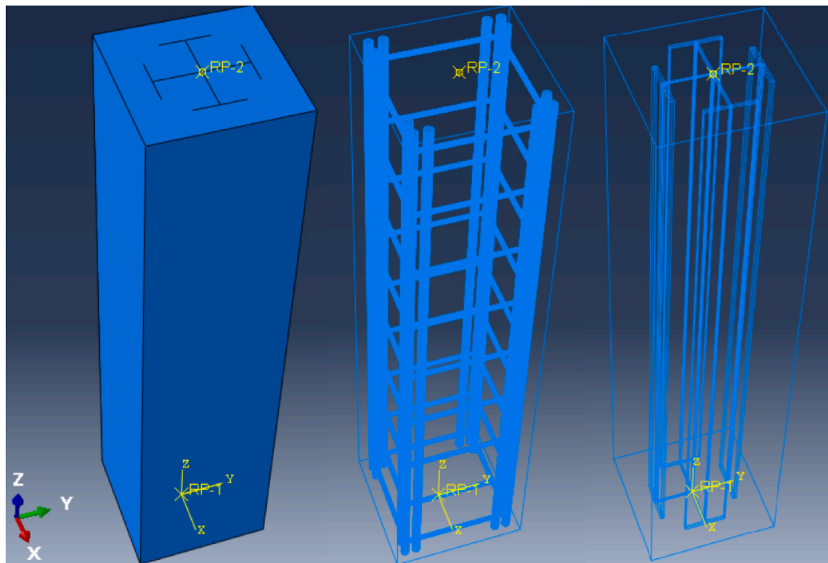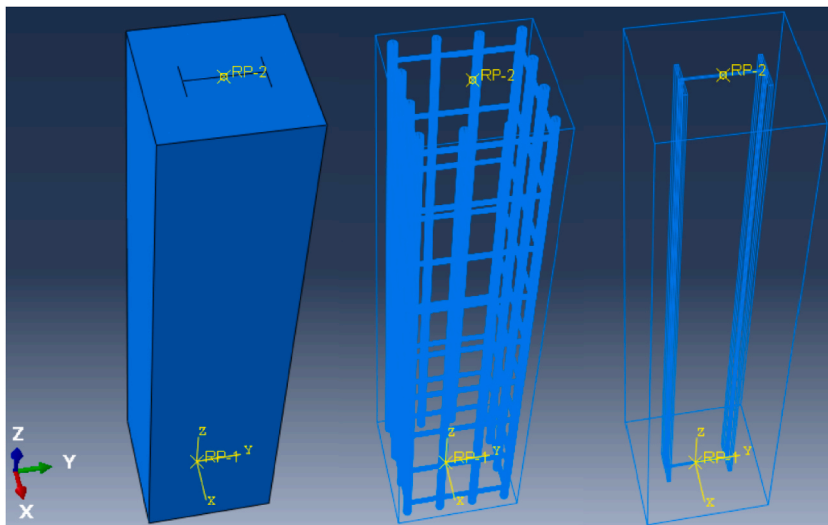
Fig. 6. 3D view of the numerical model of SRC4.

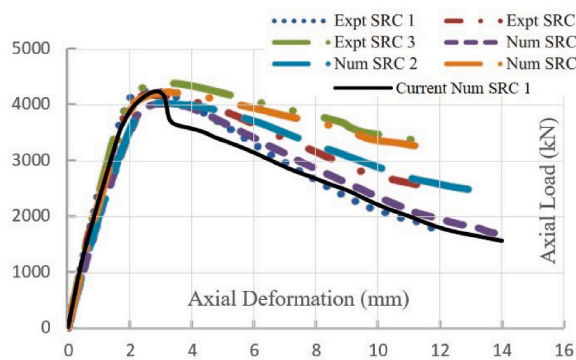**Fig. 7.** 3D view of the numerical model of SRC7.

Fig. 8. Curves obtained from experimental results [16], and validation curve from ABAQUS. (1 mm = 0.04in, 1 KN = 0.225Kips).

Table 1
Comparison between experimental and numerical results for SRC4. (1 mm = 0.04in, 1 KN = 0.225Kips).

Experimental		Numerical	
U (Displacement) mm	F KN	U (Displacement) mm	F KN
3.18	4441	2.8	4656

Table 2
Comparison between experimental and numerical results for SRC7. (1 mm = 0.04in, 1 KN = 0.225Kips).

Experimental		Numerical	
U (Displacement) mm	F KN	U (Displacement) mm	F KN
2.94	3788	3.08	3785

Table 3
General Description of Specimens to be Compared (1in = 25.4 mm).

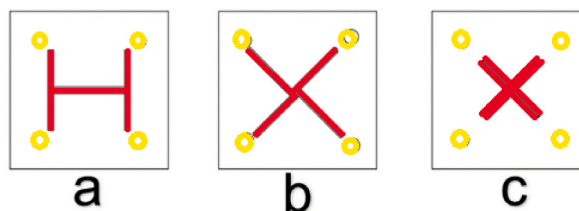|	Concrete Dimensions mm	Steel Sections (AISC)	Rebars mm
Specimen 1	200 × 200 × 1830	W100 × 330	4#10
Specimen 2	200 × 200 × 1830	2 L89 × 76.5 × 8	4#10
Specimen 3	200 × 200 × 1830	4 L50 × 50 × 6.5	4#10

Fig. 9. AutoCAD Schematic Drawing of the Specimens to be Compared. (a) Specimen 1, conventional composite concrete steel column with "W" steel column embedded. (b) Specimen 2, composite concrete steel column with 2 "L" steel angles embedded. (c) Specimen 3, composite steel column with 4 "L" steel angles embedded.

compared to determine which section had the greatest compressive strength capacity.

Steel angle sections were used solely to represent the "X" shape, and if steel fabricators have a pre-made mold for this shape, there will be no need for steel angles and welding costs during future experiments or on-site construction.

4. Results and discussion

4.1. Using AISC

Table 4 below shows the values of compressive strength of all three specimens of conventional steel section W100 × 330, two angles 2 L 89 × 76.5 × 8, and four angles 4 L 50 × 50 × 6.5.

Fig. 10 below shows that the compressive strength of the 2 L section (specimen 2) is greater than the compressive strength of the W and 4 L section, with a capacity around 20 MPa higher than the W section and higher than 4 L section. The W section shows a 62 MPa higher capacity than the 4Lsection, which can be considered comparable and similar values. It is worth noting that increasing the area of steel or modifying the "X" shape can lead to a stronger section. However, in this paper, we limited our study to only three sections (W, 2 L and 4 L) and did not explore other possibilities.

4.2. Using Eurocode4

Table 5 below shows the material properties as per Eurocode 4 [11], and values of compressive strength of all three specimens of conventional steel section W100 × 330, two angles 2 L 89 × 76.5 × 8 and four angles 4 L 50 × 50 × 6.5.

Fig. 11 below, shows that 2 L and W sections have the same compressive strength and are larger with a 6.9 MPa difference than the 4 L section.

Table 4
Compressive strength values of three specimens using AISC Chapter I Section 12. (1 KN = 0.225 Kips).

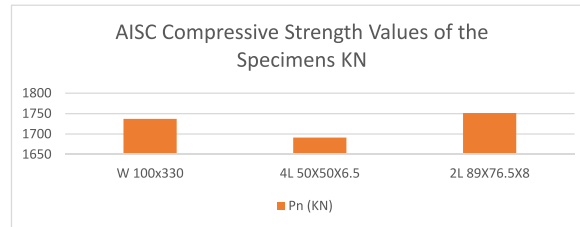|	W 100 × 330	4 L 50 × 50 × 6.5	2 L 89 × 76.5 × 8
Pn (KN)	**1737**	**1691.2**	**1751.4**

Fig. 10. Aisc compressive strength values of the specimens (1 KN = 0.225Kips).

Table 5
Compressive strength values of three specimens using Eurocode4 Section 6.71KN = 0.225Kips).

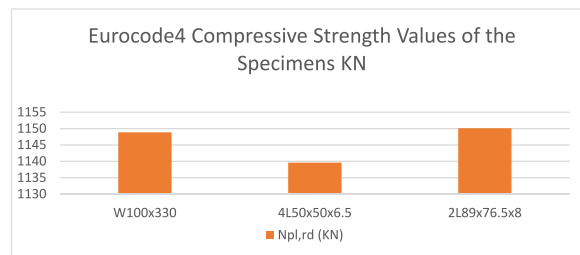| Strength	W100 × 330	4L50 × 50 × 6.5	2L89 × 76.5 × 8
Npl,rd (KN)	**1148.837**	**1139.58**	**1150.08**

Fig. 11. Eurocode4 compressive strength values of the specimens (1 KN = 0.225Kips).

4.3. Using ABAQUS

Table 6 and Fig. 12 show the Reaction forces representing the compressive strength of the three specimens after reaching the 25.4 mm (1-inch) deflection.

The specimens did not reach failure due to the displacement control approach that was used in ABAQUS. This is because these forces are applied to reach a displacement of 25.4 mm only. The goal of the simulation is to find the load which will cause 25.4 mm displacement, then calculate the reaction force.

Four angles show similar or less compressive strength than the conventional "W" section, while the two angles show greater compressive strength than the conventional "W" section and 4 L section as in theoretical analysis (sections 3.1 and 3.2). Using two angles is better based on the software analysis but it is used with care, because using a 2 L section requires having a larger sectional depth and creates a limitation on the size of the column, for example, the 2 L steel section used is 150 mm in depth and width while the "W" and 4 L steel sections are 100 mm in depth and width.

Table 6
Forces a failure of the specimens in ABAQUS. (1 mm = 0.04in, 1 KN = 0.225Kips).

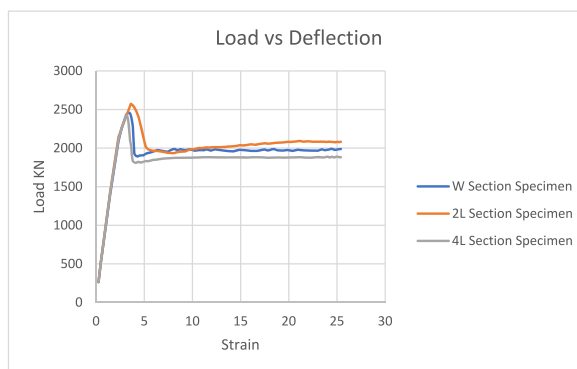| Specimens	Force at failure KN	Displacement mm
W 100 × 330	**2.45**	**25.4**
2 L 89 × 76.5 × 8	**2.58**	**25.4**
4 L 50 × 50 × 6.5	**2.42**	**25.4**

Fig. 12. Comparison of Load vs Deflection of all Specimens (1 mm = 0.04in, 1 KN = 0.225Kips).

5. Conclusion

- A new "X" steel section shape was introduced, using steel angles of the shape "L" to represent the geometry of the proposed section, since the "X" shape section is new to the industry and did not exist before:
- Finite elements analysis using the software ABAQUS and theoretical analysis using methods from AISC and Eurocode manuals were done on three concrete-steel composite columns samples W100 × 330, two angles 2L89 × 76.5 × 8 and four angles 4L50 × 50 × 6.5.
- A validation of ABAQUS finite element analysis was done on a previously published experiment. The results showed a good agreement between the experimental and numerical results using the same proposed finite element analysis for the proposed "X" steel section.
- Compressive strength values from AISC and Eurocode 4 theoretical analysis are comparable, both indicated that the "W" section and "X" section have relatively similar values.
- The finite element analysis showed that the "W" and "X" sections have relatively similar failure loads when reaching the same deflection value.
- The limitation of using steel angles to represent the "X" shape affected the results because the dimensions of the shape "X" were limited to the predefined dimensions of steel angles according to the AISC steel section dimension in the AISC manual.
- Studying more sections than the chosen three specimens in this paper will reduce the limitation and give a better understanding of the "X" steel section behavior.

Declaration of data availability

Data will be available upon request.

CRediT authorship contribution statement

Ahmad Zeyad Abu Sharea: Data curation, Formal analysis, Funding acquisition, Investigation, Methodology, Project administration, Resources, Software, Supervision, Validation, Visualization, Writing – original draft, Writing – review & editing. **Shideh Shadravan:** Supervision.

Declaration of competing interest

The authors declare the following financial interests/personal relationships which may be considered as potential competing interests:

Ahmad Abu Sharea has patent (New Steel Section "X Shape") pending to Patent Disclosure 2021-046. The patent disclosure was given by the University of Oklahoma.

Appendices.

Appendix A. (List of Equations)

$$Pn = Pno * \left(0.658^{(Pno/Pe)}\right) \qquad\qquad \text{Eq. (A.1)}$$

$$Pn = 0.877 * Pe \qquad \text{Eq. (A.2)}$$

$$Pno = Fy * As + Fysr * Asr + 0.85 * fc' * Ac \qquad \text{Eq. (A.3)}$$

$$Pe = \pi^2 (\text{EI}eff)/Lc^2 \qquad \text{Eq. (A.4)}$$

$$Ec = wc^{1.5} * \sqrt{fc'}, ksi \left(0.043 * wc^{1.5} * \sqrt{fc'}MPa \qquad \text{Eq. (A.5)}\right.$$

$$\text{EI}eff = Es * Is + Es * Isr + C1 * Ec * Ic \qquad \text{Eq. (A.6)}$$

$$C1 = 0.25 + 3 * (As + Asr / Ag) \leq 0.7 \qquad \text{Eq. (A.7)}$$

$$Npl, Rd = Aa * fyd + 0.85 * Ac * fcd + As * fsd \qquad \text{Eq. (A.8)}$$

Pe = elastic critical buckling load = $\pi^2(\text{EI}eff)/Lc^2$ – Eq. (A.4).
Ac = area of concrete, in^2. (mm^2).
As = cross-sectional area of steel section, in^2. (mm^2).
Ec = modulus of elasticity of concrete = $wc^{1.5} * \sqrt{fc'}, ksi$ ($0.043 * wc^{1.5} * \sqrt{fc'}MPa$ –
Eq. (A.5).
EIeff = effective stiffness of composite section, kip-in^2. (N-mm^2). = $Es * Is + Es * Isr + C1 * Ec * Ic$ - Eq. (A.6).
C1 = coefficient for calculation of effective rigidity of an encased composite compression member = $0.25 + 3 * (As + Asr / Ag) \leq 0.7$
- Eq. (A.7).
Es = modulus of elasticity of steel = 29,000 ksi (200,000 MPa).
Fy = specified minimum yield stress of steel section, ksi (MPa).
Fysr = specified minimum yield stress of reinforcing bars, ksi (MPa).
Ic = moment of inertia of the concrete section about the elastic neutral axis of the composite section, in⁴ (mm⁴).
Is = moment of inertia of steel shape about the elastic neutral axis if the composite section, in⁴ (mm⁴).
Isr = moment of inertia of reinforcing bars about the elastic neutral axis of the composite section, in⁴ (mm⁴).
K = effective length factor.
L = laterally unbraced length of the member, in. (mm).
Lc = K*L = effective length of the member, in. (mm).
fc' = specified compressive strength of concrete, ksi (MPa).
wc = weight of concrete per unit volume ($90 \leq wc \leq 155$ Ib/ft^3 or $1500 \leq wc \leq 2800$ kg/m^3).

References

[1] D.L. Samarakkody, D.P. Thambiratanam, T. Chan, P. Moragaspitiya, Different axial shortening and its effects in high rise buildings with composite concrete filled tube columns, Construct. Build. Mater. 143 (2017) 659–672.
[2] H.-S. Park, B. Kwon, Y. Shin, Y. Kim, T. Hong, S.W. Choi, Cost and CO2 emission optimization of steel reinforced concrete columns in high-rise buildings, Energies 6 (11) (2013) 5609–5624.
[3] M. Yarnold, E. Stoddard, Future hot-rolled asymmetrical steel I-beams, Journal of Structural Engineering 146 (9) (2020).
[4] R. Landolfo, A. Formisano, G. Lorenzo, On the origin of I beam and quick analysis on the structural efficiency of hot-rolled steel members, Cross Mark 11 (Suppl-1) (2017) 332–344. M3.
[5] A.I.o.S.C. Aisc, Specification for Structural Steel Buildings, American Institute of Steel Construction AISC, Illinois, 2016.
[6] R.Q. Bridge, M.D. O'Shea, Behaviour of thin-walled steel box sections with or without internal restraint, J. Constructional Steel Res. 47 (1–2) (1998) 73–91.
[7] M. Elchalakani, X.-L. Zhao, Concrete-filled cold-formed circular steel tubes subjected to variable amplitude cyclic pure bending, Eng. Struct. 30 (2) (2008) 287–299.
[8] C.D. Goode, A. Kuranovas, A.K. Kvedaras, Buckling of slender composite concrete-filled steel columns, J. Civ. Eng. Manag. 16 (2) (2010) 230–236.
[9] G. Campione, RC columns strengthened with steel angles and battens: experimental results and design procedure, Pract. Period. Struct. Des. Construct. 18 (1) (2013) 1–11.
[10] H.-J. Hwang, Prefabricated steel-reinforced concrete composite column, in: H. Yalciner (Ed.), New Trends in Structural Engineering, IntechOpen, 2018, pp. 60–75.
[11] E.C. f. S, Eurocode4, Eurocode 4: Design of Composite Steel and Concrete Structures, The European Union: European Committee for Standarization, Eurocode4, 2004.
[12] E. Ellobody, B. Young, Numerical simulation of concrete encased steel composite columns, J. Constructional Steel Res. 67 (2) (2011) 211–222.
[13] E. Ellobody, B. Young, D. Lam, Eccentrically loaded concrete encased steel composite columns, Thin-Walled Struct. 49 (1) (2011) 53–65.
[14] A. Lelkes, Š. Gramblička, Theoritical and experimental studies on composite steel concrete columns, Procedia Eng. 65 (2013) 405–410.
[15] ABAQUS, Standard User Maual ABAQUS V, 6.19, ABAQUS Inc, USA, 2019.
[16] M.S. Rahman, M. Begum, R. Ahsan, Comparison between experimental and numerical studies of fully encased composite columns, International Journal of Structural and Construction Engineering 10 (6) (2016).

Further reading

[17] M. Sabau, T. Onet, Nonlinear concrete behavior, Journal of Applied Engineering Sciences 1 (4) (2011) 55–60.

[18] T.-S. Eom, H.-J. Hwang, H.-G. Park, M. Asce, C.-N. Lee, H.-S. Kim, Flexural test for steel-concrete composite members using prefabricated steel angles, J. Struct. Eng. 140 (4) (2014).

[19] A.-y. Jiang, W.-l. Jin, Experimemntal investigation and design of thin-walled concrete-filled steel tubes subject to bending, Thin-Walled Struct. (2013) 44–50.

[20] L.-H. Han, G.-H. Yao, Z. Tao, Performance of concrete-filled thin-walled steel tubes under pure torsion, Thin-Walled Struct. 45 (1) (2007) 24–35.

[21] S. Tokgoz, C. Dundar, Tests of eccentrically loaded L-shaped section steel fibre high strength reinforced concrete and composite columns, Eng. Struct. 38 (2012) 134–141.

[22] C.-S. Kim, H.-G. Park, M. Asce, K.-S. Chung, I.-R. Choi, Eccentric axial load capacity of high-strength steel-concrete composite columns of various sectional shapes, J. Struct. Eng. 140 (4) (2014).

[23] G.J. Timoshenko, Mechanics of Materials, fourth ed. ed., PWS, 1997.

[24] M. Labibzadeh, M. Zakeri, A.A. Shoaib, A new method for CDP input parameter identification of the ABAQUS software guaranteeing uniqueness and precision, International Journal of Structural Integrity 8 (2) (2017).

[25] K.-H. Chu, D.J. Carreira, Stress-strain relationship for plain concrete in compression, ACI Journal (1985) 797–804.